An Automatic Method to Determine Cutoff Frequency Based on Image Power Spectrum

J. S. Beis, A. Celler, and J. S. Barney

Abstract—**We present an algorithm for automatically choosing filter cutoff frequency (F_C) using the power spectrum of the projections. The method is based on the assumption that the expectation of the image power spectrum is the sum of the expectation of the blurred object power spectrum (dominant at low frequencies) plus a constant value due to Poisson noise. By considering the discrete components of the noise-dominated high-frequency spectrum as a Gaussian distribution $N(\mu, \sigma)$, the Student t-test determines F_C as the highest frequency for which the image frequency components are unlikely to be drawn from $N(\mu, \sigma)$. The method is general and can be applied to any filter. In this work, we tested the approach using the Metz restoration filter on simulated, phantom, and patient data with good results. Quantitative performance of the technique was evaluated by plotting recovery coefficient (RC) versus NMSE of reconstructed images.**

I. Introduction

DIGITAL filtering in SPECT is often used to improve the quality of the reconstructed images. Statistical noise, due to an insufficient number of events, generally requires smoothing with a lowpass filter. Some compensation for camera blur is also possible by the use of an inverse filter. Unfortunately, these two goals are in opposition: the lowpass filter attenuates nonzero frequencies, whereas the inverse filter enhances them.

Restoration filters attempt to strike a compromise, combining smoothing and compensation into one filter. They use a parameter known as cutoff frequency, F_c, to trade off the camera blurring correction with noise suppression. The optimal value of F_c is characteristic for a given image, depending on the number of counts, camera and acquisition parameters, and the activity distribution.

In nonquantitative SPECT, subjective tests such as viewer preference may be used to determine an "optimal" cutoff. For quantitative studies, it is important to have an objective algorithm to calculate F_c and a means to quantify the effects of filtering on count totals, since changing F_c changes the distribution of counts in the image.

In this paper we present an algorithm for automatically choosing the filter cutoff frequency based on the power spectrum of the projections. A statistical test is used to determine the point at which noise begins to dominate in the higher-frequency portion of the spectrum. Using this method, an appropriate F_c can be objectively determined for each study.

Manuscript received November 15, 1994; revised August 10, 1995. This work was supported in part by MRC under Grant UI12360.

J. S. Beis is with the Department of Computer Science, University of British Columbia, and the Division of Nuclear Medicine, Vancouver Hospital and Health Sciences Center, Vancouver, B.C., Canada.

A. Celler and J. S. Barney are with the Division of Nuclear Medicine, Vancouver Hospital and Health Sciences Center, Vancouver, B.C., Canada.

IEEE Log Number 9415677.

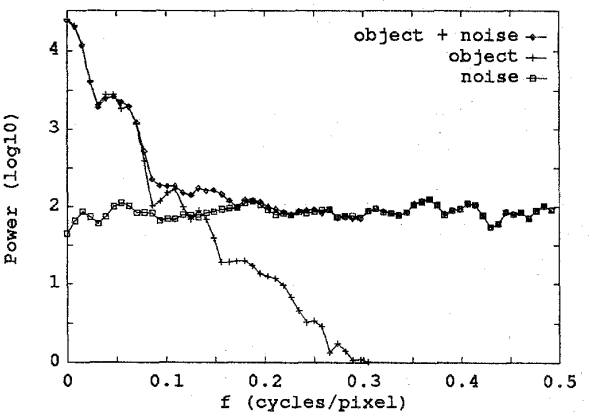

Fig. 1. Power spectra averaged over all projections for a synthetic data set of 4 spheres with radii 1, 2, 3, and 4 cm (arrangement of spheres given in Section 3). The noise level correspond to 10^4 total counts in all projections.

The Metz filter is used as a testbed, although the approach is general and can be applied to other types of filter. The quantitative performance of the algorithm is investigated using the method of Celler *et al.* [1], which considers both the recovery coefficient (RC) and the normalized mean square error (NMSE) within regions of interest.

II. Automatic Determination of F_c

Goodman and Belsher [2] showed theoretically that, for images subject to Poisson statistics, the expectation of the image power spectrum is equal to the expectation of the blurred object power spectrum plus a constant mean level due to the noise. King *et al.* [3], using synthetic data, demonstrated that the model works extremely well when the actual noise spectrum is used instead of a constant mean. As an example of this, Fig. 1 presents a synthetic image power spectrum (object + noise) broken down into its components. A set of 1-D projections was used (corresponding to a single slice), and the spectrum shown was computed by averaging the 1-D power spectra of all projections.

The analysis of Goodman and Belsher implies that the noise power spectrum should be roughly flat over the full range of frequencies. This appears to be a good approximation, both from King's results and our own experiments using synthetic

data. Furthermore, the power spectrum of the blurred object is clearly concentrated in the low frequencies because of the nature of the camera Modulation Transfer Function (MTF), which acts as a lowpass filter. The object spectrum shown in Fig. 1 demonstrates a steady (and steep) decline toward the high frequencies.

These properties, together with the realization that the total object power will always be much greater than the total noise power, suggest that as we move from high to low frequencies, there must be a point at which the object power rises above that of the noise. In the combined spectrum (object + noise), this corresponds to the point where the spectrum can no longer be considered flat, and this point will be taken to be F_c.

To locate this rise, our method requires two assumptions. The first, following the discussion in the previous paragraphs, is that the object's power spectrum above a certain frequency is negligible with respect to the noise. The second is that the components of the noise power spectrum are normally distributed about their mean value. To see why this is so, first note that each frequency component of the noise power spectra of the projections follows a χ^2 distribution with 2 degrees of freedom [4], [5]. Then, by averaging over the projection set, the Central Limit Theorem implies that the resulting noise distribution should be approximately Gaussian. Application of a χ^2 test of goodness-of-fit to our synthetic data (e.g., noise spectrum in Fig. 1) generally found reduced χ^2 values close to 1.0, verifying the theoretical result. Given these assumptions, and using the high-frequency components of the spectrum as samples, the mean and standard deviation of the noise considered as a normal distribution $N(\mu, \sigma)$ can be estimated using the standard formulas. In this paper, the upper 25% of the frequency range is used to generate samples.

A moving window is then used to generate sample sets of 10 consecutive discrete frequency components. The t-test checks the likelihood that the samples might be drawn from $N(\mu, \sigma)$. Specifically, if $\overline{x}$ is the samples mean calculated from a 10-component window, and s the corresponding variance, then $t(\overline{x}, s, N)$ is the probability that a set of 10 samples drawn from N would give a mean of $\overline{x}$ or larger.

The window is stepped down one component at a time, from high to low frequencies. The highest-frequency window for which t falls below a preset significance level, α, is the transition area between the object- and the noise-dominated regions. Its center is chosen as F_c.

This method is similar to one described in King, *et al.* [3], [5]. The main advantage here is the use of many samples in the statistical test instead of a single component. This makes the test robust in case of spurious noise fluctuations. It allows the detection of situations in which the power in the transition region rises slowly above the noise level, by taking into account not only the mean of the test sample, but the variance as well. Finally, sharp rises will be detected, due to the rapidly diverging mean.

There are two parameters that affect the value chosen for F_c: size of sampling window, and significance level α for the statistical test. The choice for both of these must accommodate the same tradeoff, between the desire to detect the rise in the object power as early as possible (i.e., at the highest appropriate frequency) versus the need to avoid detecting a large noise fluctuation.

A smaller window size localizes F_c better, but is more sensitive to noise fluctuations. Since only a fraction of the contained samples need to be correlated to one side of the mean for t to become very small, a minimal window size of perhaps 6 or 8 components must be used, regardless of the matrix size, for stability. Similarly, a larger value for α detects smaller deviations from the mean μ, finding a slightly higher value for the true cutoff, but also being erroneously triggered by smaller deviations in the noise spectrum. Considering the amount of noise generally present in clinical SPECT images, we have chosen conservative values: a 10 component window (about 16% of the 64-component spectra used throughout this work) and $\alpha = 0.01$.

III. Experiments

The restoration filter used in this study was the Metz filter [6]. It takes the form

$$Metz(f) = \frac{[1 - (1 - MTF^2(f))^X]}{MTF(f)}.$$

The Metz cutoff is controlled by the parameter X, so once F_c was computed by our algorithm, X was set such that the filter had a value of 1.0 at F_c. This assured that frequencies below F_c were amplified, and those above were damped.

The power spectrum used in the significance tests to determine F_c was the average of the 1-D power spectra of all projections comprising the slice to be reconstructed. The algorithm was tested on simulated, phantom, and patient data. Because the method we used to assess performance required ground truth images for comparison, in the following we focus primarily on the synthetic data.

The synthetic data set consisted of 4 spheres of radii 1, 2, 3, and 4 cm. The sphere centers were coplanar (in the plane of reconstruction), each one placed 8 cm from the camera rotation axis and separated by 90° from one another within the plane. A set of 64 1-D projections was generated, and convolved with a Gaussian (1 cm FWHM) to simulate camera blurring. The same Gaussian was used as the point spread function to calculate the MTF used in the Metz filter formula. The total number of counts in all projections, 10^4, is consistent with those found in patient brain studies. Finally, Poisson noise was added to each pixel in the projections.

Since true count distributions are available when synthetic data are used, it is possible to assess image quality for a given choice of filter and cutoff frequency. In quantitative studies, an important measure of the quality of reconstructions is the recovery coefficient (RC). The RC is the fraction of number of recovered image counts in a region of interest (ROI) divided by the true number of counts in that ROI. The ROI used for our RC calculations was equal to the true size of the object. Unfortunately, RC does not tell the whole story. It is possible to obtain a "perfect" result (RC = 1) for some very poor image reconstructions, for the two reasons illustrated in Fig. 2. The first is if there are large errors outside the ROI; the second is if large errors inside the ROI cancel each other out.

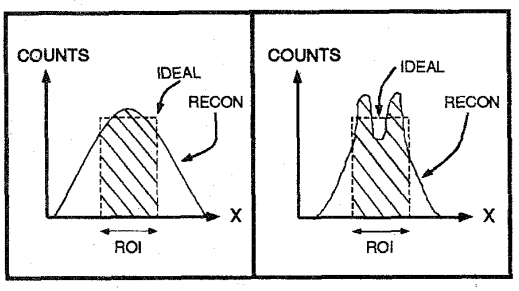

Fig. 2. Constructed examples of 1-D images showing problems with RC. Left: RC = 1, but the image quality is poor because errors outside ROI are ignored. The low contrast is likely due to too much smoothing. Right: RC = 1, but the image quality is poor because errors inside RC cancel out. The poor fidelity is likely due to low statistics or filtering artifacts.

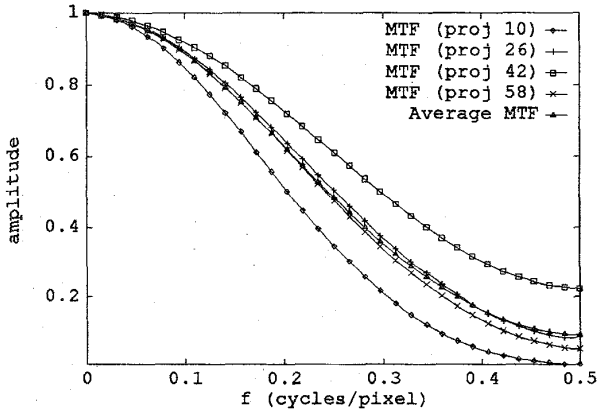

Fig. 3. Modulation Transfer Functions derived from 4 projections of a point source (see text). The average of the MTF's is also shown.

A measure that does not ignore such errors, and provides information about noise and contrast, is the NMSE, which is a pixel-by-pixel absolute difference between the reconstructed and ideal images. The NMSE has its own problems, however, in that it includes errors from regions of the image far from any objects of interest. This makes it a weak indicator of good reconstructions over localized areas. To mitigate this shortcoming, we calculate NMSE for our synthetic data using nonoverlapping ROI's with radii that are slightly larger (by 2 cm) than the true object size. The ROI must be larger than the interior of the objects to penalize any loss of contrast between the hot objects and the cold background.

To assess our algorithm's choice for F_c for the synthetic data, a method which makes use of both measures [1] was used. For a given filter, curves of RC versus NMSE over a range of F_c were generated. Any choice of F_c implicitly corresponds to some trade-offs with respect to smoothing of noise, restoration of counts, etc. Locating the choice for F_c on an RC/NMSE curve makes clear the directions in which these tradeoffs are being decided.

In addition to synthetic data, we were also interested in testing the algorithm on experimentally obtained data. In order to apply the Metz filter to phantom and patient data, the MTF for each imaging situation is required. The MTF depends on the camera characteristics, collimator type, photon energy, and

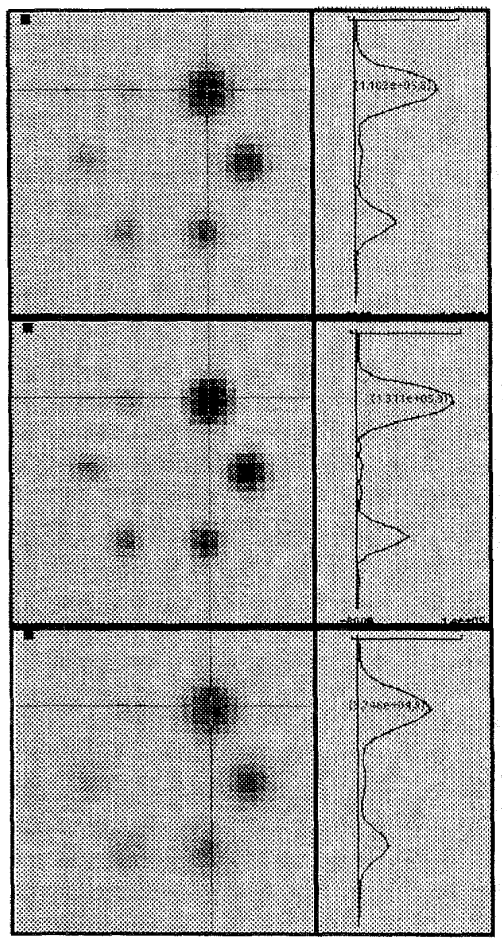

Fig. 4. Reconstructions of the Jaszczak phantom (hot Tc-99m spheres in air): unfiltered (top), Metz filtered (center), and Hann $F_c = 0.45$ cycles/pixel filtered (bottom). To the right is a profile through the center of the largest sphere, corresponding to the vertical line in each image. The data were acquired on a DST Sopha camera using HIRES collimator, a 64×64 matrix, and 64 projections.

scatter medium. Because our images were either acquired in air (Jaszczak phantom) or scatter corrected beforehand (brain study), scatter was not included in our analysis. For each of our test situations, a high-count image of a point source in air was acquired. The source was offset from the camera axis by 7 cm, in order that the distance dependence of the MTF could be observed. Four separate MTF's were computed using point spread functions from four different projections: source closest to camera; source furthest from camera; and the two projections 90° on either side of these. Fig. 3 shows the MTF's and their average for a Sopha DST camera with a HIRES collimator and Tc-99m source. The average MTF is used in the Metz filter formula above, for processing the phantom data of Fig. 4. A similar MTF is generated for use with the patient data of Fig. 5 (ADAC camera, LEGP collimator, Tl-201 source).

For objects of intermediate distances, the MTF is clearly adequate. For objects close to or far from the camera, this choice will introduce some error. Note, however, that restoration takes

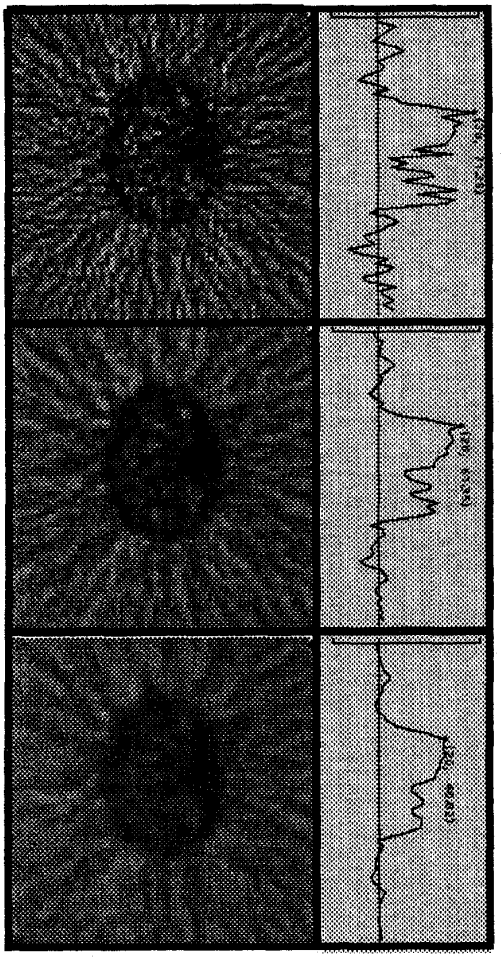

Fig. 5. Tl-201 brain study reconstructions: unfiltered (top), Metz filtered (center), and Hann $F_c = 0.45$ cycles/pixel filtered (bottom). Shown to the right of each image is a profile through the center of the highest count region, corresponding to the vertical line in each image. The data were acquired on an ADAC camera using LEGP collimator, a 64×64 matrix, and 64 projections. Attenuation and scatter correction were applied before filtering.

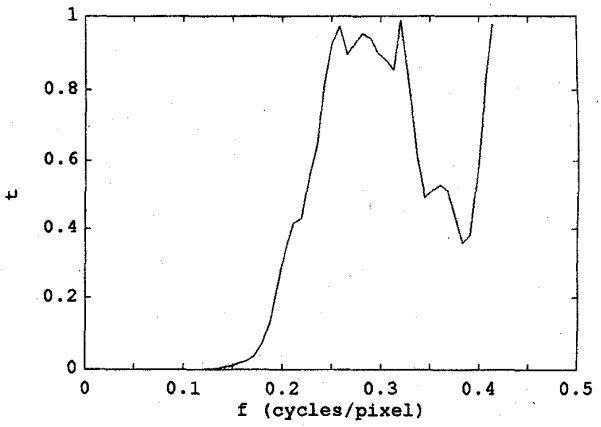

Fig. 6. Student t-test statistic for window centered at frequency f, based on the power spectrum of Fig. 1.

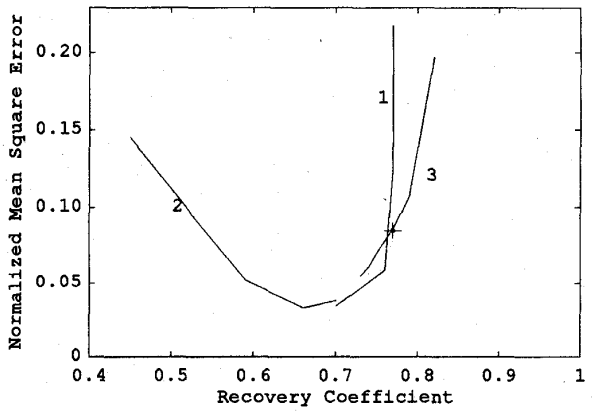

Fig. 7. RC versus NMSE for (1) rectangular, (2) Hann, and (3) Metz filters for various ranges of F_c (see text). The cross on the Metz curve indicates the filter chosen by our algorithm.

place in the lower-frequency region where the percentage differences between the average and extreme MTF's are lowest.

Our phantom data were acquired using the Jaszczak phantom (Fig. 4), in a configuration of 6 hot spheres in air (diameters 13, 16, 18.5, 25.5, 31.5, and 38 mm). The sphere centers were coplanar, at a distance of 5.2 cm from the camera axis, and spaced at equal angles (60°) from one another. The slice reconstructed in Fig. 4 contained a total of 4.9×10^6 counts.

Patient data from ^{201}Tl brain studies with between 3700 and 18,500 counts per slice were also tested. Reconstructions of a higher-count projection set are presented in Fig. 5.

IV. Discussion

Application of the automatic cutoff method to the synthetic data power spectrum determined F_c to be 0.13 cycles/pixel (corresponding to Metz parameter $X = 1.52$). Fig. 6 is a plot of the Student t-test statistic t, versus f, for this data set. A comparison of Fig. 1 and Fig. 6 shows that the point where t drops below $\alpha = 0.01$ is precisely where the object power rises above the noise power spectrum. Furthermore, there is only a short region of ambiguity, within which t is of order 0.01. Below this, it drops to an infinitesimal value and remains there. Above this region, t rises sharply toward value 1.0, supporting the hypothesis that the noise power is dominating and has a constant mean.

To assess this choice of F_c, RC versus NMSE curves were generated (Fig. 7) for the following filters and ranges of F_c. i) Rectangular—a sharp cutoff, lowpass filter, for $0.15 < F_c < 0.45$ cycles/pixel. ii) Hann—a smoothing lowpass filter, for $0.15 < F_c < 0.45$ cycles/pixel. iii) Metz—a restoration filter for $0.05 < F_c < 0.3$ cycles/pixel.

Note here that the meaning of F_c is not consistent across filter types. The rectangular filter passes all frequencies below F_c perfectly and removes all those above F_c. The Hann drops smoothly to zero at F_c, with significant damping below F_c.

The Metz amplifies below F_c, while above it still passes significant amounts of signal as it drops toward zero.

From left to right, the curves move from lower to higher F_c. Both the RC and NMSE are summed over all four of the synthetic spheres. The plots clarify the tradeoff between restoration (roughly, good RC) and image fidelity (good NMSE). It is possible to get higher values for RC by increasing F_c, and it is known that for these synthetic images RC should equal 1. However, the large NMSE values above a certain value of RC tell us that such reconstructions are poor, due either to an overall bias within the ROI, the fluctuations away from the true distribution from noise and reconstruction artifacts, or both. Observations of reconstructions indicate that, in the high-RC region of the graph, the NMSE is dominated by the noise deviations (see, e.g., the right side of Fig. 2).

The automatic choice for F_c is indicated by a cross on the Metz curve. The position of this point is a good compromise between a high value of RC and low noise level. Beyond this point, NMSE increases rapidly for small gains in RC, with the corresponding reconstructions having reduced accuracy, and becoming less and less open to visual interpretation.

The phantom study (Fig. 4) represents clearly the advantage of restoration filtering. More counts are recovered in the hot regions of the Metz filtered image than in the others, demonstrating that the smoothing is more than compensated for by the inverse MTF portion of the filter. Not only are the absolute numbers in each sphere increased, but the count ratios (Table I) between the centers of the smaller spheres and that of the largest are increased (i.e., closer to 1.0), which is appropriate since the spheres did contain identical densities of activity.

The patient reconstructions (Fig. 5) show that the filtered images are more visually pleasing. In this case, while much of the effect of the Metz filter is smoothing, it still achieves a compromise between the oversmoothed Hann $F_c = 0.45$ cycles/pixel filtered image and the high noise unfiltered image.

TABLE I
RATIOS OF PEAK NUMBER OF COUNTS IN CENTERS OF SPHERES OF VARIOUS SIZES VERSUS PEAK NUMBER OF COUNTS IN CENTER OF LARGEST SPHERE FOR METZ FILTERED, UNFILTERED, HANN FILTERED IMAGES. THE ACTUAL NUMBER OF COUNTS IN THE LARGEST SPHERE CENTERS WERE METZ: 1.31×10^5; UNFILTERED: 1.10×10^5; HANN: 0.98×10^5

	Metz	Unfilt	Hann
38.0	1.0	1.0	1.0
31.5	.87	.82	.72
25.5	.70	.63	.49
18.5	.44	.39	.27
16.0	.30	.27	.18
13.0	.20	.18	.11

V. CONCLUSION

We have presented an automatic method for determining filter cutoff frequency using a statistical test on the power spectrum of the projections. Analysis demonstrates that the approach provides a cutoff that is a good compromise between high recovery coefficient and low noise in the reconstructed image.

As stated earlier, the value of F_c chosen by this algorithm could be used with a variety of filters. Restoration filters can set their filter value to 1.0 at F_c. To generate lowpass filters, since they never rise above 1.0, another choice such as setting the filter half-power point to F_c would be appropriate. Obviously this would achieve a different tradeoff in the sense of Fig. 7 (see Hann curve as an example of a lowpass filter). Such a choice would emphasize smoothing over count recovery, perhaps desirable if the sole analysis of the image is by human observation.

REFERENCES

[1] A. Celler, J. S. Beis, and J. S. Barney, "Effects of filters on quantitation in SPECT," in *Proc. 3rd Med. Phys. Workshop: Quantitation PET SPECT,* with *18th Annu. Western Regional Meet., SNM,* Vancouver, B.C., 1993.

[2] J. W. Goodman and J. F. Belsher, "Fundamental limitations in linear invariant restoration of atmospherically degraded images," *Imaging through Amosphere, SPIE,* vol. 75, pp. 141–154, 1976.

[3] M. A. King, P. W. Doherty, and R. B. Schwinger, "A Wiener filter for nuclear medicine images," *Med. Phys.,* vol. 10, no. 6, pp. 876–880, 1983.

[4] G. M. Jenkins and D. G. Watts, *Spectral Analysis and its Applications.* San Francisco: Holden-Day, 1968, pp. 230–234.

[5] M. A. King, S. J. Glick, B. C. Penney, R. B. Schwinger, and P. W. Doherty, "Interactive visual optimization of SPECT prereconstruction filtering," *J. Nucl. Med.,* vol. 28, pp. 1192–1198, 1987.

[6] C. E. Metz and R. N. Beck, "Quantitative effects of stationary linear image processing on noise and resolution of structure in radionuclide images," *J. Nucl. Med.,* vol. 15, pp. 1234–1240, 1974.